Intermetallics 30 (2012) 30–34

Contents lists available at SciVerse ScienceDirect

Intermetallics

journal homepage: www.elsevier.com/locate/intermet

Superplastic-like deformation in metallic amorphous/crystalline nanolayered micropillars

M.C. Liu [a], X.H. Du [a,b], I.C. Lin [a], H.J. Pei [a], J.C. Huang [a,*]

[a] Department of Materials and Optoelectronic Science, Center for Nanoscience and Nanotechnology, National Sun Yat-Sen University, Kaohsiung 804, Taiwan, ROC
[b] School of Materials Sciences and Engineering, Shenyang Aerospace University, Shenyang 110034, PR China

ARTICLE INFO

Article history:
Available online 27 April 2012

Keywords:
A. Nanostructured intermetallics
B. Superplastic behaviour
C. Thin films
C. Vapour deposition
F. Mechanical testing

ABSTRACT

In this study, the ZrCu thin film metallic glasses (TFMGs) are incorporated with soft Cu thin film layers with optimum film layer thickness. Such multilayered amorphous/crystalline samples exhibit superplastic-like homogeneous deformation at room temperature. It is found that the deformability of the resultant micropillars depends on the thickness of Cu layers. Microstructural observations and theoretical analysis suggest that the superplastic-like deformation mode is attributed to homogeneous co-deformation of amorphous ZrCu and nanocrystalline Cu layers because the 100-nm-thick Cu layers can provide compatible flow stress and "plastic zone" size well matched with those of ZrCu amorphous layers.

1. Introduction

Recently, several studies have revealed that metallic amorphous/crystalline nanolayered composites (MACNCs) have the capacity of simultaneously sustaining large plasticity and high strength at room temperature , making MACNCs promising in making nano- or micro-scaled devices, which are pervasive in modern industries [1–3]. For MACNCs, to manufacture small-dimension devices with complex shapes, superplastic forming at low or even room temperature has been commonly accepted as one of the most feasible as well as economic methods for light metals [4,5]. This fact makes it of great interest to explore the possibility of MACNCs to sustain intrinsically superplastic-like flow at room temperature.

An inspired fact is that some amorphous and nanocrystalline materials have inherently the capacity of superplastic-like deformation behavior under uniaxial compression [6–8]. From mechanical viewpoints, two factors beneficial to obtain the superplastic-like deformation of MACNCs are suggested: (a) matched capacity of plastic deformation between nanoscaled amorphous and crystalline layers, and (b) perfect strain compatibility at amorphous/crystalline interfaces. Here, the strain compatibility is not a problem for the amorphous/crystalline interfaces owing to their positive roles as high-capacity sinks for dislocations, by which unique inelastic shear (slip) transfer properties are caused [2,3]. Therefore, how to achieve the matched plastic deformation capacity between nanoscaled amorphous and crystalline layers becomes the crucial issue to obtain homogeneous deformation for MACNCs. For bulk metallic glass composites, large compressive plasticity [9,10] and tensile ductility [11,12] have been explored by matching the length scale of glassy phase with the "plastic zone" size, providing an opportunity to pursue the matched mechanical properties between amorphous/crystalline layers by tailoring their microstructural scale.

Furthermore, our recent works [1,13] on amorphous ZrCu with ductile metallic crystalline underlayers (Cu or Zr) show that the toughening effects depends on the thickness values of crystalline metallic underlayers. Similar observation of the modulation period effect of ductile Cu layers on toughness has also been reported recently in crystalline-Cu/crystalline-Cr multilayered films [14]. The results reveal that the deformation behavior of metallic multilayered materials is related directly to the thickness of ductile metallic layers. In this study, metallic amorphous ZrCu/crystalline Cu nanolayered micropillars are chosen to systematically investigate the effect of modulating ductile Cu layer thickness on their deformation behavior.

2. Experimental details

Amorphous ZrCu/crystalline Cu multilayered thin films were deposited alternately on Si (100) wafers by magnetron sputtering. The thickness of amorphous ZrCu layer was fixed at 100 nm and the

* Corresponding author. Tel.: +886 7 525 2000x4063; fax: +886 7 5254099.
E-mail address: jacobc@mail.nsysu.edu.tw (J.C. Huang).

0966-9795/$ – see front matter © 2012 Elsevier Ltd. All rights reserved.
doi:10.1016/j.intermet.2012.03.037

thickness of crystalline Cu layer was changed from 10, 25, 50, 75, to 100 nm. The resultant multilayered thin films are denoted as 100/10, 100/25, 100/50, 100/75, and 100/100 ZrCu/Cu in this paper, respectively. The total thickness of ZrCu/Cu multilayer films is about 2500 nm. Moreover, the monolithic amorphous ZrCu thin films were also prepared for comparison. The nature of as-deposited thin films was characterized by X-ray diffraction (XRD, Siemens), field-emission scanning electron microscopy (SEM, JEOL-6330), and transmission electron microscopy (TEM, JOEL 3010). To further explore the micro-scaled mechanical properties of the as-deposited thin films, micropillars were prepared from the deposited films using the dual focus ion beam system (FIB, Seiko SMI3050 SE). Detailed descriptions about the micropillars preparation procedures and testing methods have been described elsewhere [15,16].

In this study, round and rectangle micropillars were employed to evaluate the deformation behavior of ZrCu/Cu multilayer films. The round micropillars have a diameter of 1 μm and effective height of about 2.5 μm with a taper angle of about 3°. To reduce the taper effect, rectangle micropillars with cross-sectional area of around 1.3 × 1.3 μm and effective height of 2.5 μm were also prepared. The taper angle in the rectangle microplillars can be successfully reduced to less than 0.7°. Therefore, the influence of taper angle during microcompression testing and datum analysis can be minimized. Microcompression tests were performed on the micropillar samples with a nanoindentation system (MTS nanoindenter XP) under the loading rate control mode using a flat punch tip with an equilateral triangle cross-section measuring 13.5 μm in side length, which was also machined out of a standard Berkovich indenter by FIB in the continuous stiffness measurement (CSM) mode. While displacement was reached, the nanoindenter system has a short period of holding time, about 10 s. The morphology of micropillar before and after deformation was examined by SEM. Furthermore, to observe the detailed shear band interactions in multilayer micropillar samples after deformation, TEM samples were fabricated by FIB, using a trenching and liftout technique.

3. Results and discussion

Fig. 1 shows a TEM micrograph of the 100/100 ZrCu/Cu round multilayered micropillar, in which the brighter and darker contrast corresponds to the amorphous ZrCu layers and nanocrystalline Cu layers, respectively. The average equiaxed grain size of nanocrystalline Cu layers is about 30–50 nm.

The SEM micrographs of the deformed monolithic amorphous ZrCu, 500/500, 100/10 and 100/100 ZrCu/Cu nanolayered micropillars are presented in Fig. 2(a)–(d). The corresponding engineering stress-strain curves are shown in Fig. 2(e) (the 500/500 pillar results were presented in our earlier paper) [13]. As shown in Fig. 2(e), the curve for the monolithic amorphous ZrCu micropillar exhibited pronounced strain bursts at ~2.6 GPa, indicative of sudden propagation of shear events [17,18] and consistent with the SEM observations in Fig. 2(a), where shear bands were obviously observed. Fig. 2(e) also shows the curve for the 500/500 micropillar, however, the main strain was carried out by the deformation of Cu layers in which severe-barreling shape appeared in Fig. 2(b). This pillar yielded at about 1.2 GPa, the yield strength of nanocrystalline Cu, and exhibited work hardening associated with the deformation of the Cu layer. Even though the Cu layer was plastically deformed, the amorphous phase was still in the elastic range, thereby no shear band could be initiated in the amorphous layer.

For the 100/10 ZrCu/Cu multilayer micropillars, although the stress-strain curve showed a bend-over phenomenon before the strain burst event, the deformation was still dominated by the emission of shear bands in a manner of strain burst, which was evidenced by SEM observations shown in Fig. 3(c). This means that with increasing Cu layer thickness, the elastic-to-shear transition becomes more gradual. This should be caused firstly by the deformation and work hardening of the 10 nm Cu layers, followed by the shear band initiation in the ZrCu layers upon the system flow stress reaching the ZrCu yield stress. Following this trend, for the 100/100 micropillar, a smooth curve with no noticeable strain burst is recorded in Fig. 2(e). The multilayered pillar exhibited a yield strength of ~2.3 GPa with an overall plastic engineering strain above 20%. Since the lower portion is basically undeformed, the original upper half (~1.3 μm in height and ~0.9 μm in diameter) has been compressed to ~0.6 μm in height and ~1.3 μm in diameter. This means that the upper half has experienced a compressive engineering strain in height of ~50%, an increment of cross-section of ~110% or a true strain of ~0.75. Note that the 100/100 micropillars did not fail after such extensive compressive straining, as shown in Fig. 2(d).

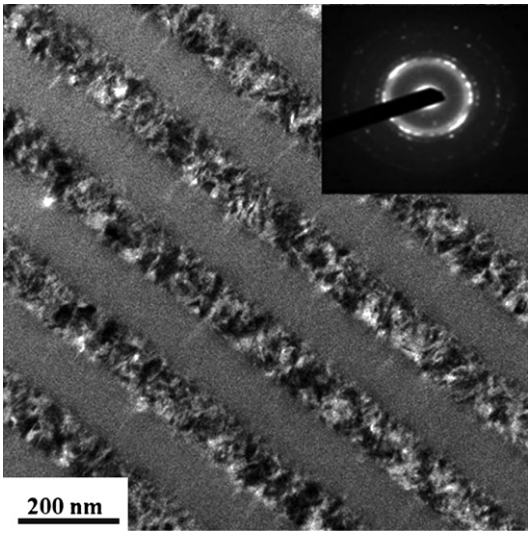

Fig. 1. Bright-field TEM micrograph showing the microstructure of the 100/100 ZrCu/Cu multilayer thin films. Insert shows the corresponding selected area electron diffraction pattern.

To further demonstrate the compressibility of the 100/100 ZrCu/Cu micropillar without the taper angle effect, rectangle micropillars with a taper angle less than 0.7° were tested. The SEM micrographs of micropillars before and after compressive straining are shown in Fig. 3(a) and (b). The original rectangle micropillar has been compressed significantly to multilayered pan-cake appearance. The corresponding true stress-true strain curve is shown in Fig. 3(c), presenting the superplastic-like flow behavior at room temperature with a compressive engineering strain in height of ~70%, increment of cross-section of ~160% or a true strain of ~1.0.

These results show that the deformation of ZrCu/Cu nanolayered micropillars depends significantly on the thickness of ductile Cu layers under uniaxial microcompression conditions. It is interesting to note that the critical metallic thickness of Cu layers for the superplastic-like flow is around 100 nm, equal to the thickness of amorphous ZrCu layers. To further characterize the deformation features of 100/100 ZrCu/Cu multilayered micropillars, the longitudinal section of the compressed micropillars were examined by TEM, as shown in Fig. 4. By measuring the final thickness of the severely strained ZrCu or Cu layers (some drop to 10 nm from the original unformed thickness of 100 nm), the local engineering strain in height can be as high as ~90% or a true strain of ~2.3. Multiple shear events could be observed in the thicker amorphous ZrCu layers. No shear events can be observed in the thinner amorphous

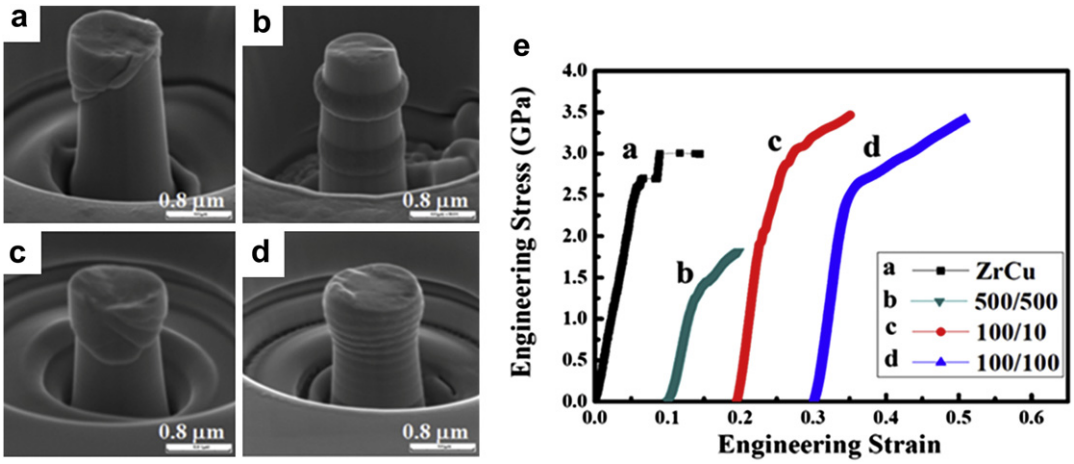

Fig. 2. SEM micrographs showing the appearance of the round deformed micropillars: (a) monolithic amorphous ZrCu, (b) 500/500, (c) 100/10, and (d) 100/100 ZrCu/Cu micropillar. The engineering strain-stress curves of these four specimens are shown in (e).

ZrCu layers due to the merging effect of pronounced plastic deformation to the shear events. Nevertheless, for the deformed 100/100 ZrCu/Cu micropillar, semi-homogeneous deformation occurred in both the nanocrystalline Cu and amorphous ZrCu layers. This means the shear cracks have been effectively suppressed during compression for the 100/100 ones. The Cu layers should still undergo conventional dislocation movements causing the strain hardening behavior as observed in Fig. 3(c).

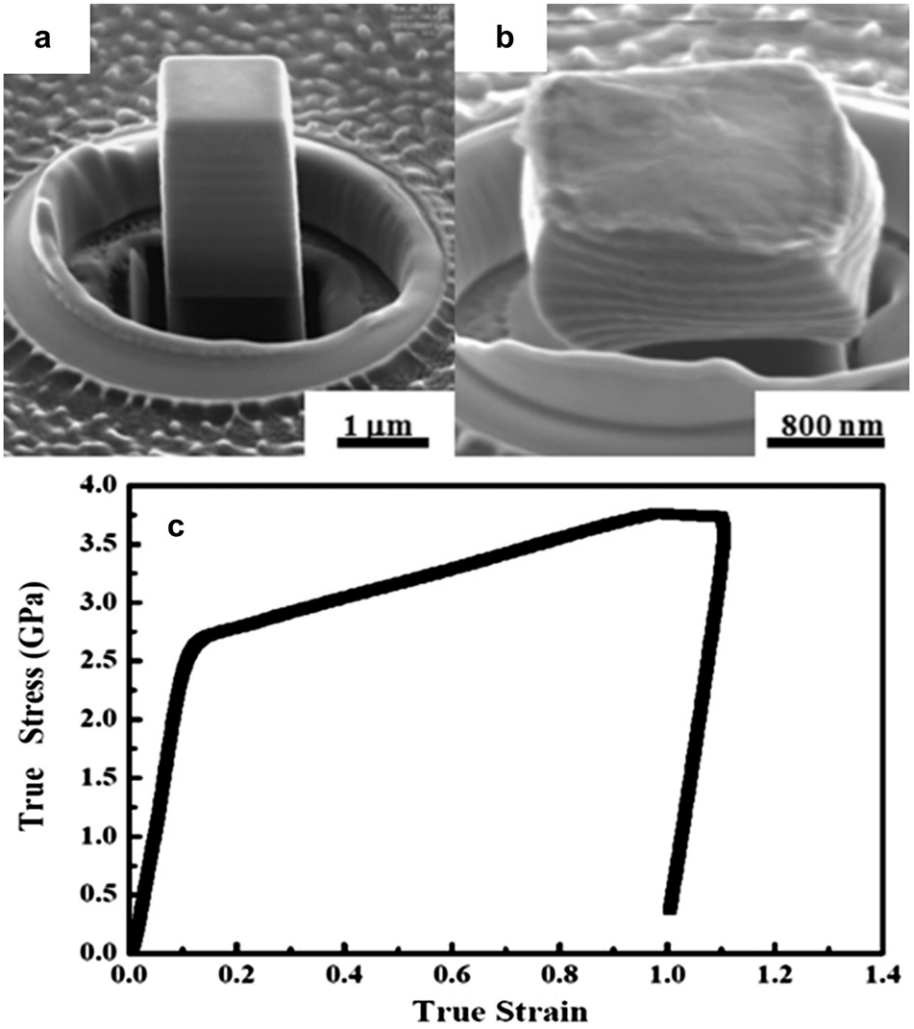

Fig. 3. SEM micrographs showing the appearances of the (a) undeformed and (b) strained up to ~100% 100/100 ZrCu/Cu rectangular micropillars. (c) A typical curve of 100/100 ZrCu/Cu rectangular micropillars subjected to microcompression test.

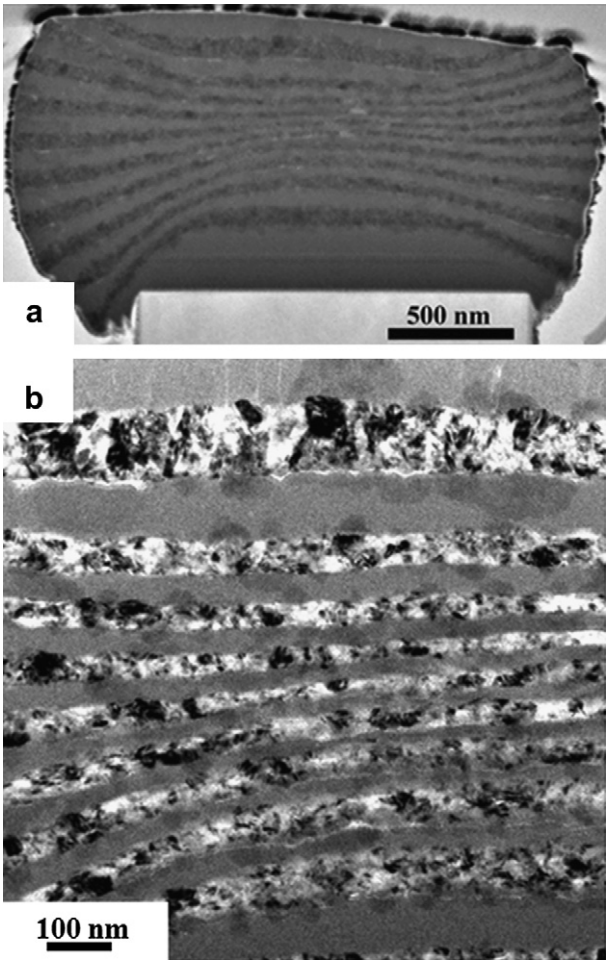

Fig. 4. TEM micrographs showing the appearances of the deformed 100/100 ZrCu/Cu rectangular micropillars.

Before discussing the physical mechanism underlying the superplastic-like behavior of 100/100 nanolayered micropillars, it is required to define the flow behavior characteristics of the amorphous layers for 100/100 micropillars during superplastic-like deformation process. This can be done by a rough estimate on the value of the average Newtonian viscosity η. By using the approximate strain rate of 8×10^{-4} s^{-1}, and a stress level of 3.5 GPa, the viscosity can be calculated to be 1.5×10^{12} N s/m^2 (or Pa s) by the equation of $\eta = \sigma/3\dot{\varepsilon}$, where σ is stress and $\dot{\varepsilon}$ is strain rate. Obviously, this value is at least one order higher than that of the typical viscosity for metallic glass materials near the glass transitions [19], meaning that the deformation of glassy layers is performed mainly by multiple shear events rather than homogenous movement of minor defects, such as free volumes. This is consistent with the TEM observations, as shown in Fig. 4(b).

Due to the "shear events" controlled deformation, suppression of compressive instability for the 100/100 micropillar requires an operative mechanism to restrict the shear events to evolve into shear cracks. On one hand, the introduction of ductile Cu layers can provide the microstructual possibility to toughen the micropillar. On the other hand, under uniaxial compression, the amorphous ZrCu and crystalline Cu layers are subjected to tensile and compressive stress, respectively, owing to the preferential extension along the lateral direction for the softer Cu metallic layers. The existence of interior stress gradient is beneficial for the multilayerd micropillars to exhibit plastic deformation ability, similar to the case of bending thin metallic amorphous plates [20,21]. In this case, the high-stiffness ZrCu amorphous layers could become the effective geometric objects to hamper the propagation of shear bands initiated around the plastically soft objects, i.e. the amorphous ZrCu/crystalline Cu interfaces.

Bending produces an inherently inhomogeneous stress state where a shear band is arrested by the gradient in applied stress, $\Delta\sigma = 2\sigma_y/D$. Here, the σ_y is the yield stress and D is the thickness of the bending plate. Stability against crack opening is geometrically ensured when $D/2 < R_p$ [20,21], where R_p is the size of plastic zone. Thus, following this fundamental concept, it is reasonable to derive that if the thickness of ZrCu glassy phase L_a, i.e., the distance for shear bands propagation, becomes comparable with the plastic zone size, i.e, $L_a \leqq R_p$, the extension of shear band can be arrested. This concept has been exploited to design ductile bulk metallic glasses composites [9–12].

The plastic zone size of metallic amorphous/crystalline nanolayered micropillars can be estimated by analogizing shear events as minor crack propagation. For a mode I opening crack, the characteristic dimension R_p of a crack tip plastic zone can be expressed as [22]:

$$R_p = K_{IC}^2/2\pi\sigma_Y^2, \tag{1}$$

where K_{IC} is plain-strain fracture toughness. In a laminate consisting of alternative brittle and ductile layers, the crack extension resistance is enhanced as the thickness of metal layers increases, thus, a critical value of the stress intensity factor, i.e. the plain-strain fracture toughness, can be estimated by [23],

$$K_{IC} \approx \sigma_Y\sqrt{2\pi L_m}, \tag{2}$$

where L_m is the thickness of plastic metal layers. Therefore, combining eqns. (1) and (2), the plastic zone size of the amorphous/metallic laminates can be given by:

$$R_p \approx L_m. \tag{3}$$

This means that the plastic zone of amorphous/crystalline multilayered micropillars equals to the thickness of plastically crystalline layers, consistent perfectly with the experimental observation of this study. The condition with $R_p \approx L_m$ will provide the matched plastic deformation ability between amorphous ZrCu and nanocrystalline Cu layers. Thus, one of necessary conditions for amorphous/metallic multilayered micropillars to deform plastically is that the thickness of amorphous layers should be comparable or less than that of metallic layers, i.e., $L_a \leqq L_m$.

To satisfy strain compatibility at the crystalline/amorphous interface, the metallic Cu layers must have matched flow stress with the amorphous ZrCu layers. Several researches have suggested that for the metallic layers thicker than a few tens of nanometer, the plastic deformation can be assisted by mechanical advantage of dislocations pile-ups, in which the Hall-Petch relationship between flow stress σ and the thickness of layers L_m is available, i.e., $\sigma \propto L_m^{-1/2}$ [24]. This provides an opportunity for the Cu layer to achieve matched mechanical properties with amorphous ZrCu layer by changing its thickness. From our current experimental results, 100 nm appears to be the right thickness range for metallic Cu layers to reach the matched flow stress with that of amorphous ZrCu layer. For the metallic Cu layers with the thickness much lower than 100 nm, such as 10 or 20 nm, the confined layer slip (CLS) behavior would result in the stress scales much higher than that of amorphous ZrCu layers. In this case, the shear bands initiated in the ZrCu layers would pass through the whole specimens (based on the model by Cao and Evans [23]), resulting in compression instability, as observed in Fig. 2(c). Otherwise, if the thickness of metallic Cu

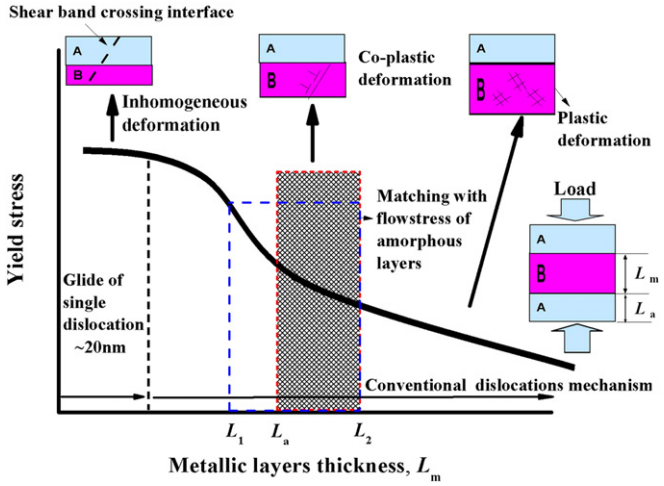

Fig. 5. Schematic illustration of the deformation mechanism in the metallic amorphous/crystalline nanolayered composites as a function of metallic layers thickness. A: inherently ductile metallic amorphous layers (e.g. ZrCu) with L_a thickness; B: soft pure metallic layers (e.g. Cu). Pronounced semi-homogeneous and superplastic-like deformation can occur when $L_a \leqq L_m \leqq L_2$.

layers is much higher than 100 nm, such as 500 nm in this study, the ultra low flow stress of metallic Cu layers with respect to that of amorphous ZrCu layers would make the pillar deformation basically carried only by the Cu layers, leaving ZrCu unchanged, as observed in Fig. 2(b).

To explain the unusual superplastic-like plasticity of 100/100 ZrCu/Cu nanolayered micropillars, the relationship between of mechanical properties and thickness between metallic and amorphous layers is schematically illustrated in Fig. 5. We can estimate the thickness range of metallic layers giving rise to a matched strength with that of the amorphous layers. For the current ZrCu amorphous layer, the yield stress is about 2–2.5 GPa (a sharp burst will initiate at ~2.6 GPa). With the concept of $\sigma \propto L_m^{-1/2}$ [24] for the crystalline Cu metal layer, we can define a length scale range from L_1 to L_2 for the Cu layer to possess a similar flow stress of 2.0–2.5 GPa. Based on our experience, L_1 and L_2 for the current case are about 80 and 150 nm, respectively. As demonstrated in Fig. 5, the metal layer with a thickness less than 20 nm would lead to inhomogeneous deformation in both the amorphous and crystalline layers. The metal layer with a thickness between L_1 and L_2 (within the blue dashed square in Fig. 5) would ensure matched flow stresses of the metal and amorphous layers, leading to co-plastic deformation of both layers. Coupled with the requirement based on foregoing analysis from Eqns. (1)–(3), namely, $L_a \leqq L_m$, the optimum crystalline metal layer thickness should satisfy the relationship, $L_a \leqq L_m \leqq L_2$, as demonstrated in the shaded area in Fig. 5. Under this condition, superplastic-like homogeneous and co-deformation mode to large strains is possible.

4. Conclusions

In summary, to design superplastic-like amorphous/crystalline nanolayered micropillars, one might choose amorphous forming alloys or TFMGs coupled with pure soft metals (such as Cu, Al, Ag, Au, Pd) with high deformation capacity in room temperature. Beside, the two basic principles should be followed: (1) modulating the thickness of metal layers to ensure their flow stress of metallic layers matched with that of amorphous layers ($L_1 \leqq L_m \leqq L_2$); (2) presetting the thickness of amorphous layers equal or less than that of the metallic layers ($L_a \leqq L_m$). Based on the two principles, we can derive a definite criterion, $L_a \leqq L_m \leqq L_2$, for various amorphous/crystalline multilayers to deform plastically. This strategy is expected to provide useful guidelines in designing superplastic-like amorphous/crystalline nanolayered materials used for micro-electro-mechanical systems.

Acknowledgements

The authors gratefully acknowledge the sponsorship from National Science Council of Taiwan, ROC, under the project No. NSC 98-2221-E-110-035-MY3.

References

[1] Liu MC, Huang JC, Chou HS, Lai YH, Lee CJ, Nieh TG. Scripta Mater 2009;61:840–3.
[2] Donohue A, Spaepen F, Hoagland RG, Misra A. Appl Phys Lett 2007;91:241905.
[3] Wang YM, Li J, Hamza AV, Barbee Jr TW. Proc Natl Acad Sci U.S.A (PNAS) 2007;104:11155–60.
[4] Huang JC, Chuang TH. Mater Chem Phys 1999;57:195–206.
[5] Wang YN, Huang JC. Scripta Mater 2003;48:1117–22.
[6] Liu YH, Wang G, Wang RJ, Zhao DQ, Pan MX, Wang WH. Science 2007;315:1385–8.
[7] Pan D, Kuwano S, Fujita T, Chen MW. Nano Lett 2007;7:2108–11.
[8] Yao KF, Ruan F, Yang YQ, Chen N. Appl Phys Lett 2006;88:122106.
[9] Hays CC, Kim CP, Johnson WL. Phys Rev Lett 2000;84:2901–4.
[10] He G, Eckert J, Loser W, Schultz L. Nat Mater 2003;2:33–7.
[11] Hofmann DC, Suh JY, Wiest A, Duan G, Lind ML, Demetriou MD, et al. Nature 2008;451:1085–9.
[12] Hofmann DC, Suh JY, Wiest A, Lind ML, Demetriou MD, Johnson WL. Proc Natl Acad Sci U.S.A (PNAS) 2008;105:20136–40.
[13] Liu MC, Lee CJ, Lai YH, Huang JC. Thin Solid Films 2010;518:7295–9.
[14] Zhang JY, Liu G, Zhang X, Zhang GJ, Sun J, Ma E. Scripta Mater 2010;62:333–6.
[15] Lee CJ, Huang JC, Nieh TG. Appl Phys Lett 2007;91:161913.
[16] Lai YH, Lee CJ, Cheng YT, Chou HS, Chen HM, Du XH, et al. Scripta Mater 2008;58:890–3.
[17] Cheng S, Wang XL, Choo H, Liaw PK. Appl Phys Lett 2007;91:201917.
[18] Schuster BE, Wei Q, Ervin MH, Hruszkewycz SO, Miller MK, Hufnagel TC, et al. Scripta Mater 2007;57:517–20.
[19] Spaepen F. Acta Metall 1977;25:407–15.
[20] Conner RD, Johnson WL, Paton NE, Nix WD. J Appl Phys 2003;94:904–11.
[21] Conner RD, Li Y, Nix WD, Johnson WL. Acta Mater 2004;52:2429–34.
[22] Meyers MA, Chawla KK. Mechanical metallurgy: principles and Applications. Englewood. Cliffs, New Jersey: Prentice-Hall; 1984.
[23] Cao HC, Evans AC. Acta Metall 1991;39:2997–3005.
[24] Misra A, Demkowicz MJ, Wang J, Hoagland RG. JOM 2008;60:39–42.